A Novel Virtual Reality Environment for Preoperative Planning and Simulation of Image Guided Intracardiac Surgeries with Robotic Manipulators

Erol Yeniaras [a,1], Zhigang Deng [b], Mushabbar A. Syed [c], Mark G. Davies [d] and Nikolaos V. Tsekos [a]

[a] *Medical Robotics Lab., Dept. of Computer Science, University of Houston, USA*
[b] *Computer Graphics and Interactive Media Lab., Dept. of Computer Science, U. of H.*
[c] *Division of Cardiovascular Medicine, Loyola University Medical Center*
[d] *Department of Cardiovascular Surgery, The Methodist Hospital System*

Abstract. The evolution of image-guided and robot-assisted procedures can be beneficial to intracardiac interventions. This paper proposes a novel approach and a virtual reality system for preoperative planning and intraoperative guidance of cardiac procedures, and for investigating the kinematics and control of a virtual robotic manipulator, based on MRI CINE images. The system incorporates dedicated software modules for processing MR images, generating dynamic trajectories in the continuously changing environment of a beating heart, controlling a specific generic virtual manipulator along those trajectories, and a virtual reality interface that fuses all those information. The proposed system is applied for the simulation of accessing the aortic valve annulus via a small incision on the apex by maneuvering a robotic manipulator through an access corridor that safely transverses the left ventricle (LV) of the beating heart.

Keywords. MRI, medical robotics, cardiac surgery, virtual reality, image guidance

Introduction

The advent of real-time image guidance (RTIG), especially combined with controlled manipulators, offers new opportunities for volumetric manipulation and assessment of the tissue function before, during and after a procedure [1]. Potential benefits of RTIG for intracardiac procedures on the beating heart include: reduction of side effects associated with cardiopulmonary bypass, the option for assessing the results of the procedure at the natural beating condition of the heart, and the faster patient recovery [2]. Currently, three-dimensional (3D) ultrasound is the most common modality due to its real-time volumetric data collection, and lack of ionizing radiation [3, 4].

In recent years, magnetic resonance imaging (MRI) has emerged as a meritorious modality for RTIG due to the following features: (1) a plethora of contrast mechanisms for the morphological and functional assessment of heart pathology, as well as imaging

[1] Corresponding Author: Nikolaos V. Tsekos, Medical Robotics Laboratory, Department of Computer Science, Univ. of Houston, Houston, TX 77204, USA; E-mail: ntsekos@cs.uh.edu

protocols for visualizing interventional tools and robotic manipulators, (2) 3D and multislice imaging, (3) on-the-fly adjustment of the acquisition parameters directly from the robotic control core, and (4) no ionizing radiation. MRI guided interventions have evolved significantly in recent years [5] and lately MRI guidance has been demonstrated to be successful in transapical aortic valve interventions [6, 7].

In this paper, we present a novel computational methodology, and its integration into a system, for performing and simulating preoperative planning and intraoperative guidance of MRI-guided and robot-assisted intracardiac procedures on the beating heart via transapical access. In particular, the herein described system introduces:

- A dynamic virtual reality environment that provides an information-rich, intuitive and comprehensive perception of the area of procedure (AoP) to the operator based on pre- and intra-operative MRI.
- On-the-fly generation of patient-specific dynamic access corridors inside the left ventricle (LV), for the safe maneuvering of a robotic manipulator [8].
- A generic robot control based on dynamic trajectories extracted from MRI.

1. Methods

For setting the design direction of the proposed system it is instructive to first assess the specific topography related to a procedure that entails a transapical access to the aortic valve. Figure 1A shows a long axis MR image of the heart with the identified entrance point at the apex and targeted aortic annulus. As illustrated in Figure 1B and 1C, in a generalized transapical approach, the manipulator enters the heart at an apical point (P_A) and deploys inside the LV toward the targeted center of aortic annulus (P_T). Analysis of multislice MR images indicates that the deployment path of the manipulator from P_A to P_T may need to follow a non-straight path, including a deflection point (P_D) near the base of the LV. From the kinematic and path planning points of view, the major challenge is to determine the transient positions of P_A, P_D and P_T points (guiding-points) and the dynamic safe access corridor (S_C) relative to the inherent, absolute coordinate system of the MR scanner.

Considering the current simulation and potential future *in vivo* applications, this work is based on the following assumptions. First; the base of the manipulator is anchored at the apex (P_A), which is determined from CINE images, but in an *in vivo*

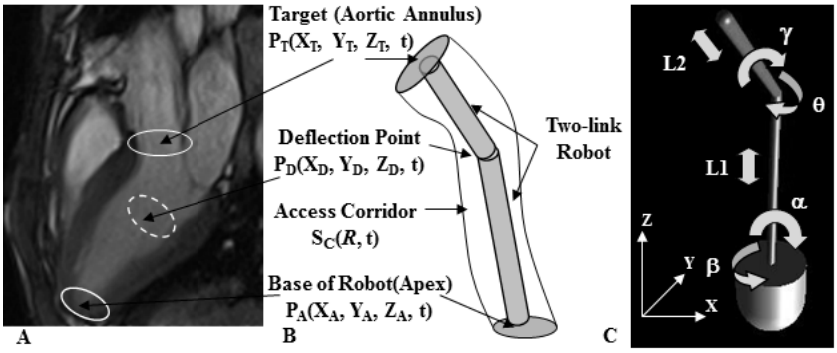

Figure 1. (A) Topography of the area of interest. (B) Representation of the deployment task. (C) A model of the virtual robot for the simulated paradigm of transapical access to the aortic valve.

scenario, miniature RF coil beacons can be attached to the base of the robot for tracking [9]. Second; S_C is both extracted and updated using multislice CINE MRI. In practice a complete CINE set will be used only preoperatively to define S_C for a complete heart-cycle, whereas a limited number of intra-oblique slices will be used to update the S_C in real-time during the procedure [6, 7]. The coordinates of P_T will also be extracted and tracked using the same limited number of slices with fast tissue tracking algorithm[10].

Figure 2 outlines the core system architecture, which will be connected to a commercial clinical MR scanner (e.g., Siemens MAGNETOM) for real-time access to the raw MR data and on-the-fly adjustment of imaging parameters[11].

1.1. MR Image Processing

The task of image processing includes the detailed segmentation of the endocardium and the identification of the three guiding-points: the apical (P_A), the mid-LV (P_D) and the targeted center of aortic annulus (P_T). Preoperative planning and the simulation are based on the datasets that were collected on healthy volunteers (n=10) with a true fast imaging, steady-state precession (TrueFISP) pulse sequence with the acquisition parameters: TR = 2.3 ms, TE = 1.4 ms, Alpha = 80^o, slice thickness = 6 mm, interslice distance = 6 mm, and acquisition matrix = 224x256. Each dataset included nineteen short and five long axes slices depicting 25 frames for a heart cycle.

The CINE datasets of short axis (SA) and long axis (LA) images were segmented to extract the LV and the aortic annulus by tracing the corresponding endocardial boundary using an in-house developed software gadget endowed with Insight Toolkit (ITK) routines. To realistically model the access corridor in LV, the segmentation contours included the papillary muscles as depicted in Figure 3A, i.e., treating them as parts of the endocardial wall since they are also obstacles to the progress of the robotic manipulator. This is in contrast to the current simplified practice in the literature that segments the LV ignoring the details of the papillary muscles.

The access corridor S_C was determined from the segmentation contours as a surface inside the LV that does not contact the endocardial wall in any time frame. In other words, *"when inside this time-dependent safe corridor, the robotic manipulator should touch neither the endocardium nor the papillary muscles"*. Using a conservative

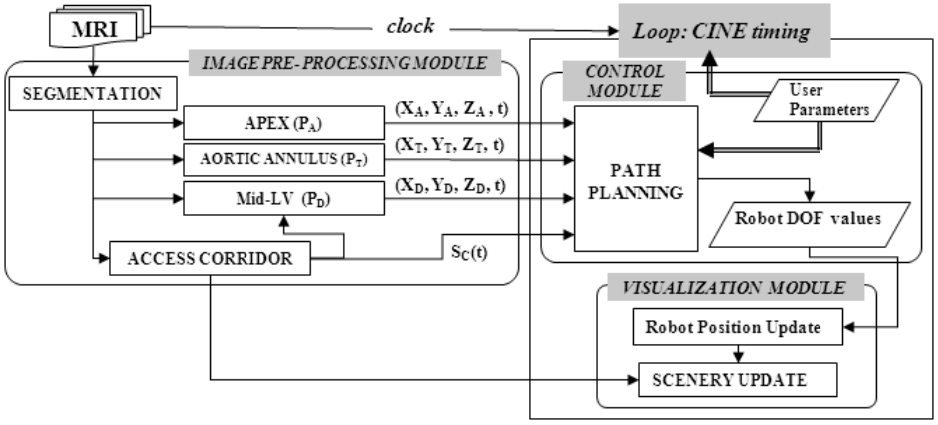

Figure 2. Flowchart of the system: the timing of the robot deployment and movement is synchronized with that of the acquisition of the CINE MR images.

approach for akinetic and dyskinetic areas, our algorithm performed the following steps for every single time frame (∀t: t=1 to 25):

1. Determine all SA slices which have a visible LV blood pool by simply checking the inside surface areas of the LV endocardial boundary contours from the apex to the base of the heart (e.g., Figure 3A and 3B). Obviously, if an area is non-zero (or bigger than a preset threshold value), the slice shows the blood pool.
2. Project LV endocardial boundary contours of these SA slices onto a single virtual plane along their common orthogonal axis to find their common area (S_B (t)) by a 2D polygon intersection algorithm. This projection is based on the fact that SA slices are parallel to each other and collected with the same field of view. Figure 3A and 3B depict all the endocardial contours and the common areas in two extreme heart phases, namely, diastole (relaxation) and systole (contraction).
3. Extend this common area, from the apex to the base of the heart, through all short axis slices to construct a straight access corridor (Figure 3C).

Since a unique 3D access corridor is generated for every single heart phase (time frame), S_C is a 4D dynamic entity for a complete heart cycle, i.e., $\exists S_C$ (t), ∀t: t=1 to 25. Further analysis of S_C showed that its average base area for 10 patients takes the maximum value of 430 mm^2 in relaxation and minimum value of 97 mm^2 in contraction which is wide enough for the safe access of a robotic catheter.

The coordinates of the apical point, P_A (t), for any time frame (t) were determined by identifying the extreme point of the apical curvature on the central long axis view, which was further verified by assessing whether it belongs to a short axis that does not depict any blood pool (i.e., it is only myocardium) for the time frame. The coordinates of the targeted point, P_T (t), were determined from the segmentation contours of two LA and one SA slices that included the aortic valve annulus at the level of the aortic valve leaflets, as the midline aortic annulus. In real life surgery, the operator can define the exact target point according to personal surgical approach to the aortic valve intervention. The deflection point for any time frame, P_D (t), was then assigned as the intersection of the aortic annulus midline (from the previous step) with the S_B (t) of the first-to-cross short axis slice. To the end, the three extracted guiding points P_A (t), P_D (t) and P_T (t) were sent to the control module while the access corridor S_C (t) was sent to the visualization module.

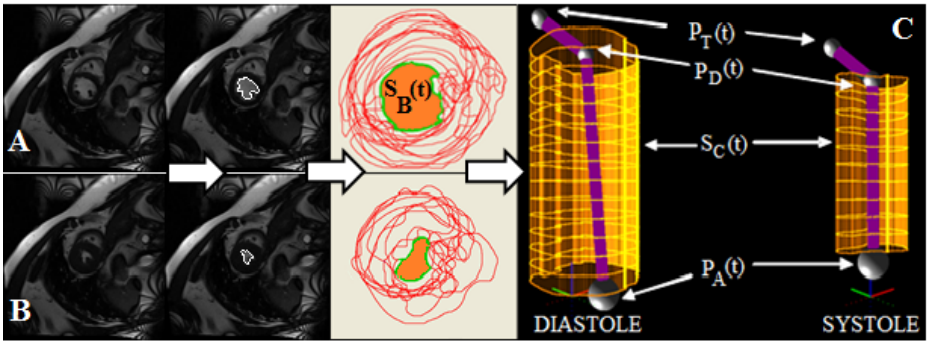

Figure 3. Methodology is depicted step-by-step. A sample short axis slice shows (A) diastole and (B) systole phases and their ITK segmentation contours. The inside of a contour is blood-pool (i.e., inside of LV). All such contours of a particular time frame are projected to a common plane and S_B (t) is found as their intersection. (C) S_B (t) is extended to define the corridor.

1.2. Control and Visualization Modules

Control module performs the inverse kinematics (IK) calculation and determines the values of six degree-of-freedom (DOF) parameters (refer to Table 1) for deploying the virtual robot from the apical point (P_A) to the targeted point (P_T) via deflection point P_D, as well as for holding its position at any intermediate or terminal arrangement specified by the operator. The inputs to this module are the dynamic coordinates of the aforementioned guiding-points P_A (t), P_D (t) and P_T (t) and the initial conditions specified by the operator; i.e., the time frame when the robot initiates its maneuvering, and whether and for how long it may hold a certain position along its path.

Table 1. IK analysis of the virtual robot (Figure 1C) at the coordinate system of MR scanner.

DOF parameter	**IK equation**
α: first Euler angle at Apical point P_A	$\alpha = \cos^{-1}((z_D - z_A)/ L_1)$
β: second Euler angle at Apical point P_A	$\beta = \cos^{-1}((x_D - x_A)/(L_1 * \sin\alpha))$
L_1: length of the first prismatic link	$L_1 = \text{sqrt}((x_D - x_A)^2 + (y_D - y_A)^2 + (z_D - z_A)^2)$
γ: first Euler angle at Mid-LV point P_D	$\gamma = \cos^{-1}((z_T - z_D)/ L_2)$
θ: second Euler angle at Mid-LV point P_D	$\theta = \cos^{-1}((x_T - x_D)/(L_2 * \sin\gamma))$
L_2: length of the second prismatic link	$L_2 = \text{sqrt}((x_T - x_D)^2 + (y_T - y_D)^2 + (z_T - z_D)^2)$

The purpose of the visualization module is to generate and update a virtual reality environment that simulates the AoP which was implemented with OpenGL. The visualization module can display any combination of the following objects: MR images, segmentation contours, guiding-points, 3D access corridor, and virtual robot. The AoP is built relative to the inherent coordinate system of the MR scanner, which offers a natural space of visualizing 3D geometric structures. The update rate of the AoP is the same as that of the collected MR images. In its basic form, the AoP can display and refresh the positions of the three guiding points as shown in Figure 4A. The access corridor may also be included with or without the manipulator. Different scenarios can be simulated to assess the beginning of a procedure, the idling of the manipulator at any instance, or the whole duration of the heart cycle.

Motion of the virtual robot entails the following three steps: deployment of the first link from the apex to the top of the LV point P_D (Figure 4A (1), (2)), extension of the second link toward the targeted point P_T, and the holding of the position (Figure 4A (3), (4)). During the maneuvering process, the control module supplies the values of the

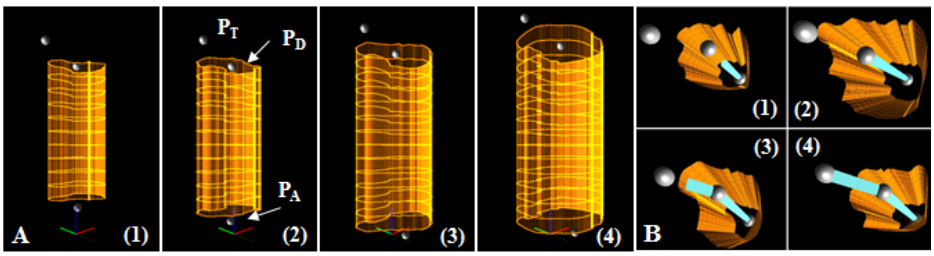

Figure 4. Four selected frames: (A) showing the access corridor and the three guiding-points which are calculated with respect to the MR scanner coordinate system and updated dynamically, (B) top view of step-by-step robot deployment within the corridor from apex to aortic annulus.

updated DOFs for each time instance. For the purpose of visualization, the intersections of P_A to P_D line with all the slices are calculated and depicted.

2. Results and Discussion

The system was successfully tested for several different combinations of: DOF actuation speeds, diameters of robotic links, numbers of simulated heart cycles, heart phases when deployment was initialized, and holding of the robot at any particular configuration. Figure 5 illustrates the actuated DOFs at a representative example of a simulated procedure. After an initial user-selected short idling period of 250 ms, the graphs reflect two phases of robot maneuvering. The Phase I is the *extension of the first link* (L_1) from the apical point P_A toward the deflection point P_D. In this phase, the rotational DOFs alpha and beta are actuated to maintain the deployed link L_1 inside the access corridor S_C and along the P_A-to-P_D line. After the distal end of the first link reaches the base point P_D, the Phase II starts immediately and entails the *extension of the second link* (L_2) to reach the targeted point P_T at the entrance of the aortic valve annulus. Concurrently, the rotational DOFs gamma and theta are also actuated to maintain the second link along the midline of the annulus. Once the annulus is reached, the robot maneuvering is performed to hold the position: the base of the robot at the apical point, the distal end of the first link at P_D, and the distal end of the second link at P_T.

In this work, preoperative planning utilized CINE MRI of several slices over a complete heart cycle to determine the diameter of the aortic annulus, the anatomy of the coronary ostia, the apical entrance point and a dynamic access corridor. Once combined with an automated segmentation algorithm[12], which is beyond the scope of this study, the system can function with a direct connection to an MR scanner and thus be able to receive MR data and control the image acquisition parameters on-the-fly.

The implemented virtual robotic manipulator was selected to offer the highest possible flexibility for performing a free-beating heart procedure. In addition to assessing the operation of the described system, this virtual tool offers a versatile kinematic structure for further investigating imaging-based path planning within dynamically changing environments, as well as approaches for automated compensation and position-holding. While many other different mechanical designs

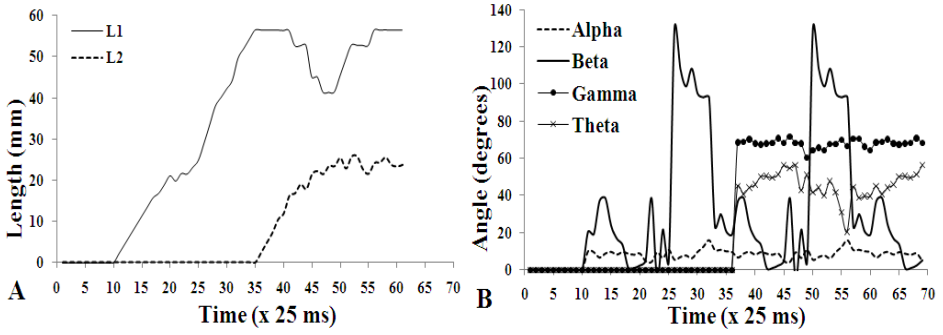

Figure 5. (A) Linear, (B) rotational DOFs of the robotic device calculated by the control module. Time (x25): 0-10: Idling period; 10-35: Phase I; 35-65: Phase II; 65- : Holding position.

may be envisioned to be more appropriate, including experimental and commercially available steerable snake-like devices such as the Hansen catheters, the proposed approach is not limited to particular technical specifications. The path planning algorithm can be adapted to any given kinematic structure.

Our preliminary studies underscore the capabilities of imaging for dynamically changing non-straight access procedures beyond the realm of endoscopy [13]. Image guidance, combined with a robotic device, may also enhance future directions in the evolution of procedures such as the Natural Orifice Transluminal Endoscopic (NOTES) and Single Port Access (SPA) surgeries [14]. Our future work includes the physical prototyping of the virtual robot presented herein and implementation of real-time MRI with mutually-oblique slices.

Acknowledgments

This work was supported by the NSF award CNS-0932272. All opinions, findings, conclusions or recommendations expressed in this work are those of the authors and do not necessarily reflect the views of our sponsors.

References

[1] F.A. Jolesz, Future perspectives for intraoperative MRI, *Neurosurg Clin N Am* **16** (2005), 201-213.
[2] P. Atluri, E.D. Kozin, W. Hiesinger, Y.J. Woo, Off-pump, minimally invasive and robotic coronary revascularization yield improved outcomes over traditional on-pump CABG, *Int J Med Robot* **5** (2009) 1-12.
[3] R. Mebarki, A. Krupa, C. Collewet, Automatic guidance of an ultrasound probe by visual servoing based on B-mode image moments, *Proceedings of MICCAI* **11** (2008), 339-346.
[4] S.G. Yuen, S.B. Kesner, N.V. Vasilyev, P.J. Del Nido, R.D. Howe, 3D ultrasound-guided motion compensation system for beating heart mitral valve repair, *Proceedings of MICCAI* **11** (2008), 711-719.
[5] N.V. Tsekos, A. Khanicheh, E. Christoforou, C. Mavroidis, Magnetic resonance-compatible robotic and mechatronics systems for image-guided interventions and rehabilitation: a review study, *Annu Rev Biomed Eng* **9** (2007), 351-387.
[6] E.R. McVeigh, M.A. Guttman, R.J. Lederman, M. Li, O. Kocaturk, T. Hunt, S. Kozlov, K.A. Horvath, Real-time interactive MRI-guided cardiac surgery: aortic valve replacement using a direct apical approach, Magn *Reson Med* **56** (2006), 958-964.
[7] M. Li, D. Mazilu, K.A. Horvath, Robotic system for transapical aortic valve replacement with MRI guidance, *Proceedings of MICCAI* **11** (2008), 476-484.
[8] E. Yeniaras, N. Navkar, M.A. Syed, N.V. Tsekos, A Computational System for Performing Robot-assisted Cardiac Surgeries with MRI Guidance, *Proceedings of SDPS* **15** (2010), 1-6.
[9] D.R. Elgort, E.Y. Wong, C.M. Hillenbrand, F.K. Wacker, J.S. Lewin, J.L. Duerk, Real-time catheter tracking and adaptive imaging, *J Magn Reson Imaging* **18** (2003), 621-626.
[10] Y. Zhou, E. Yeniaras, P. Tsiamyrtzis, N.V. Tsekos, I. Pavlidis, Collaborative Tracking for MRI-Guided Robotic Intervention on the Beating Heart, *Proceedings of MICCAI* **13** (2010), 1001-1009.
[11] E. Christoforou, E. Akbudak, A. Ozcan, M. Karanikolas, N.V. Tsekos, Performance of interventions with manipulator-driven real-time MR guidance: implementation and initial in vitro tests, *Magn Reson Imaging* **25** (2007), 69-77.
[12] M. Fradkin, C. Ciofolo, B. Mory, G. Hautvast, M. Breeuwer, Comprehensive segmentation of cine cardiac MR images, *Proceedings of MICCAI* **11** (2008), 178-185.
[13] C.A. Linte, J. Moore, C. Wedlake, D. Bainbridge, G.M. Guiraudon, D.L. Jones, T.M. Peters, Inside the beating heart: an in vivo feasibility study on fusing pre- and intra-operative imaging for minimally invasive therapy, *Int J Comput Assist Radiol Surg* **4** (2009), 113-123.
[14] J. Kobiela, T. Stefaniak, M. Mackowiak, A.J. Lachinski, Z. Sledzinski, NOTES-third generation surgery: Vain hopes or the reality of tomorrow, *Langenbecks Arch Surg* **393** (2008), 405-411.